Electricity Generation Using Vibroacoustic Coupling Between End Plate Vibrations and Internal Sound Field of Cylindrical Structure

V.G.Hamsaveni,associate professor,dept.of.EIE
N.C.Alluraiah, Assistant Professor,dept.of.EEE

Abstract:
In the present paper, we describe vibroacoustic coupling between structural vibrations and the internal sound fields of thin structures. A cylindrical structure with thin plates at both ends is considered, and the coupling between the plate vibrations and the internal sound field is obtained when an external harmonic force is applied to only one end plate. This coupling is theoretically and experimentally investigated by considering the behavior of the plates and the acoustic characteristics of the internal sound field with variations in dimensions of the structure. The dimensions and phase differences between plate vibrations, which maximize the sound pressure level inside the cavity, are clarified theoretically. These theoretical results are validated experimentally through an excitation experiment using an experimental apparatus that emulates the analytical model. Moreover, the experiment of electricity generation verifies that vibroacoustic coupling is effective in the electricity generation system adopted in this investigation, if the coupling phenomena are promoted.

Keywords: Vibroacoustic coupling, cylindrical enclosure, Structural vibration, internal sound field

1. Introduction

Thermo acoustic engines, which use the inherently efficient Stirling cycle and are designed on the basis of a simple acoustic apparatus with no moving parts, has been regard as the representative means to scavenging acoustic energy that exists in ambience1. As the example of application, electricity generation using resonance phenomena in the thermo acoustic engine was investigated with the goal of harvesting the work done in the engine. The acoustic energy spent on the generation of electricity was harvested from a resonance tube that branches out of the engine, and the appropriate position of the resonance tube for effectively generating electricity was described2. Moreover, electricity generated from the sound of a voice via piezoelectric elements was developed in order for the voice to be a supplementary electric source for a mobile phone3, and this system was being investigated for application in other devices4. Since acoustic energy is extremely small in comparison with vibration energy and the above electricity is generated by both sound and vibration systems, vibroacoustic coupling between both systems is one means of amplifying acoustic energy, although vibroacoustic coupling has not been investigated extensively in this field model to investigate coupling between the sound field in an aircraft cabin and the vibrations of the rear pressure bulkhead was proposed5,6. A cylindrical structure adopted as the analytical model, in which the rear pressure bulkhead at one end of the cylinder was assumed to be a circular plate, was examined under a variety of conditions. The plate was supported at its edges by springs, the stiffnesses of which could be adjusted to simulate various support conditions. These investigations clarified the influence of the support conditions on the sound pressure of an internal sound field coupled with the vibration of the end plate. On the other hand, in order to suppress the above vibration and acoustic energy that was amplified by vibroacoustic coupling, an analytical model that was contrived in the installation of passive devices on the vibration system was proposed as the electro-mechanical-acoustic system. The effect was fully validated in the numerical approach due to tuning resonance characteristics of the shunt circuit, in which the piezoelectric device was incorporated, to frequency characteristics of the coupling system7.In almost all such studies, vibroacoustic coupling was estimated by assuming that the plate and cavity dimensions and the phase difference between the vibroacoustics of the two plates were fixed. However, the eigenfrequencies of the plate and cavity vary with the dimensions of the plate and cavity and the phase difference directly affects the sound field when the medium is much less dense than the plate. Although a good grasp of coupling phenomena had attracted a great deal of attention, the parametric study has rarely been carried out for the above influence up to now, so that their influence on the Coupling phenomena almost remains unknown In order to develop a new electricity generation system in the present study, we herein adopt an analytical model similar to the above mentioned cylindrical structure with plates at both ends, because the vibration area of the model, on which piezoelectric elements can be installed, is twice as large as that in the case of a single plate. The dimensions of both the plate and the cylinder are varied over a wide range, while a harmonic point force is applied to only one end plate and its

frequency is selected to cause the plate to vibrate in the fundamental mode. Vibroacoustic coupling that occurs between plate vibrations and the sound field in the cavity is theoretically and experimentally investigated in terms of the vibration and acoustic characteristics. In the experiment, the acceleration of the plate vibrations, the phase difference between them, and the sound pressure level inside the cavity are considered to be significant characteristics of the plate vibrations and sound field. These experimental results demonstrate the underlying theoretical analysis on the basis of this model; conditions to maximize the vibration and sound pressure levels. Furthermore, the effect of vibroacoustic coupling is estimated from the experiment of electricity generation performed with piezoelectric elements.

2. Analytical model

The analytical model considered herein consists of a cavity with two circular end plates, as shown in Fig. 1. The plates are supported by translational and rotational springs distributed at constant intervals and the support conditions are determined by their respective spring stiffnesses, *T*1 and *T*2, and *R*1 and *R*2, where the suffixes 1 and 2 indicate plates 1 and 2, respectively. The dimensions (i.e., the radius *a* and the thickness *h*) of the plates, which have Young's modulus *E* and Poisson's ratio ɾ rare constant. The sound field is assumed to be cylindrical and to have the same radius as the plates, and the length of the sound field is assumed to vary with the cylinder length. The boundary conditions are considered to be structurally and acoustically rigid at the lateral wall between the structure and the sound field. The coordinates used are the radius *r*, the angle θ between the planes of the plates and the cross-sectional plane of the cavity, and the distance *z* along the cylinder axis. The harmonic point force *F* is applied to plate 1 at r_1 divided by *a*, and θ_1 is fixed at 0 deg. The natural Frequency of the plate is used as its excitation frequency. Moreover, the phases of the respective plates are denoted by $ø_1$ and $ø_2$ and the phase difference ø between both plate vibrations is defined as follows: $ø = ø_2 - ø_1$.

2. *Experimental apparatus and method*

Figure 2 shows the experimental apparatus used in the present study. The cylindrical structure consists of a steel cylinder with circular aluminum end plates that are 3 mm thick. The cylinder has inner radius of 153 mm, and this length can be varied from 500 to 2000 mm in order to emulate the analytical model. A harmonic point force is applied to only one end plate by a small vibrator, the amplitude of which is controlled to be 1 N. The position of the point force *r*1 is normalized by radius *a*, and the position of the point force is set to *r*1/*a* = 0.4 in the same manner as the analytical model. In the excitation experiment, the main characteristic of the plate vibration under consideration is the phase difference between the plate vibrations. Therefore, acceleration sensors are installed on both plates to measure this phase difference. In order to estimate the internal acoustic characteristics, the sound pressure level in the cavity is measured using condenser microphones with a probe tube. The respective tips of the probe tubes are located in the vicinities of the respective plates and the cylinder wall, which is the approximate location of the maximum sound pressure level as the sound field becomes resonant.

On the other hand, because electricity generation is considered as the application of this investigation, the experiment is performed with piezoelectric elements that are installed at each

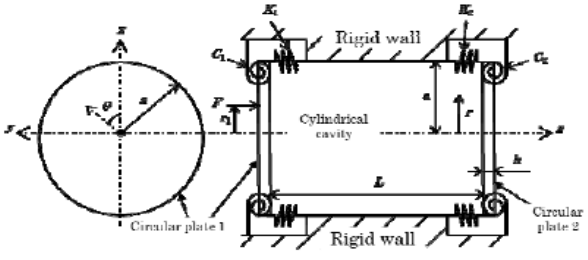

Fig. 1 ***Configuration of the analytical model***

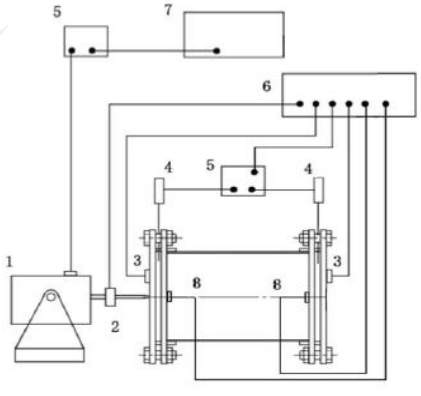

1: Vibration generator
2: Load cell
3: Acceleration sensor
4: Condenser microphone
5: Amplifier
6: FFT analyzer
7: Multifunction generator
8: Piezoelectric element

Fig. 2 ***Configuration of the experimental apparatus***

Center on not only both plates of the above structure but also both plates as the cylinder is removed from the above structure. The electric power generated by the piezoelectric elements is estimated from the relationship between the voltage of the electricity and the acceleration of the plate vibration. The effect of vibroacoustic coupling phenomena is expressed in the voltage with coupling normalized by the voltage without coupling that is harvested only from plate vibration excited by a point force

4. Results and discussion

4.1. Vibroacoustic coupling between plate vibrations and internal sound field

Figure 3 shows the sound pressure levels *Lp*1 and *Lp*2, which are, respectively, measured in the vicinities of the plate 1 and 2, as functions of *L*. The theoretical level *Lpv*, which is maximized at each *L* when the phase difference ø ranges from 0 deg to 180 deg, is also indicated To compare with these experiment results. Although these results are based on the end plates at h = 3 mm, the theoretical and experimental excitation frequencies are set to 280 and 282 Hz in order to induce the (0,0) mode. *Lp*1 and *Lp*2 that are caused by the (0,0,*q*) modes make peaks around 650, 1280, and 1880 mm and these levels are almost coincident in each peak. However, they decrease in the middle range of those lengths, in particular, decreases in *Lp*1 are remarkable and their differences expand around 950 and 1550 mm. *Lpv* also makes peaks at 610, 1230 and 1840 mm and corresponds approximately with the above lengths where *Lp*1 and *Lp*2 peaks. Figure 4 shows the distributions of sound pressure level *Lpa* averaged over a lateral cross-sectional plane (r θ plane) through the cavity along the z direction as *L* =880 and 1390 mm, around which the sound pressure level decreases. They are different from resonant distributions and behave similarly to the

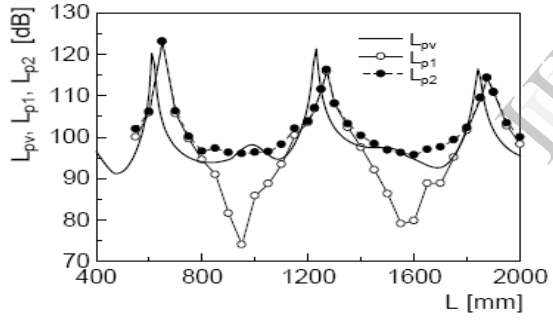

Fig. 3 ***Theoretical and experimental sound pressure levels inside cavity***

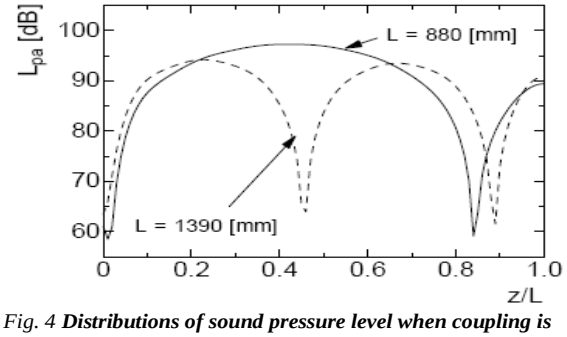

Fig. 4 ***Distributions of sound pressure level when coupling is weakened.***

sound field inside a sound tube having a single open end a single closed end. These occur in the process of shifting in acoustic modes due to changing the cylinder length and are demonstrated by the difference between *Lp*1 and *Lp*2 in the middle range of lengths at which the sound pressure level peaks.

Since the plate vibrations take part in such an acoustic characteristic via vibroacoustic coupling, the magnitude of the flexural displacements *w*1 and *w*2 is also significant in studying the effect of the plate vibrations on the sound field. Here, the phase differences are denoted by ø *max*1 and ø *max*2 when *w*1 and *w*2 are maximized, while they are denoted by ø *min*1 and ø *min*2 when *w*1 and *w*2 are minimized. Figure 5(a) and 5(b) show ø *max*1 and ø *max*2, and ø *min*1 and ø *min*2 as functions of *L*, respectively. ø *max*1 is constant at 180 deg for *L* ranging from 100 to 480 mm and decreases abruptly up to 0 deg at *L* = 490 mm. Then, ø *max*1 remains constant at 0 deg up to *L* = 620 mm, increases gradually with *L*, and returns to 180 deg at *L* = 1240 mm, increasing somewhat abruptly in the vicinity of *L* = 1080 mm. Beyond *L* = 1240 mm, ø *max*1 is again constant at 180 deg up to *L* = 1690 mm, and this behavior is repeated as *L* increases to *L* = 2000 mm. Although ø *max*2 exhibits gradual and abrupt changes that are similar to the changes in ø *max*1, the gradual and abrupt changes in ø *max*1, and ø *max*2 occur alternately. For example, in ø *max*2 when *L* increases, a gradual decrease occurs between *L* = 100 and 620 mm, and an abrupt increase occurs in the vicinity of *L* = 1080 mm. Both ø *max*1 and ø *max*2 shift between 0 and 180 deg with the change in *L* and intersect at approximately 90 deg and near the length at which *Lpv* peaked in Fig. 3. On the other hand, being similar to the changes in ø *max*1 and ø *max*2, the behavior of ø *min*1 and ø *min*2 is the exact opposite of them. In this figure, the theoretical results ø *max* at which *Lpv* peaks and the experimental results ø *exp* as *Lp*1 and *Lp*2 are maximized at each *L* are plotted. In the range of *L* except where the sound pressure level peaks, although almost all ø *exp* is in the shaded areas surrounded

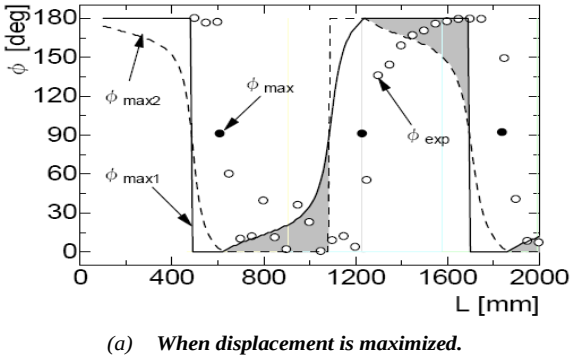

(a) ***When displacement is maximized.***

by ø *max*1 and ø *max*2, ø *exp* in the narrow range of *L* shorter than that, at which the sound pressure level peaks, is in the shaded areas surrounded by ø *min*1 and ø *min*2. Figure 6 shows the vibration levels *Lv*1 and *Lv*2 of the plates 1 and 2 as a function of *L* and the above regions of ø *min*1 and ø

*min*2 in which ø *exp* exists are represented by the shaded areas. Furthermore, the respective acceleration α1 and α2 of the plates 1 and 2 is plotted to compare with the theoretical behavior of the plates. *Lv*1 is much less than *Lv*2 in these

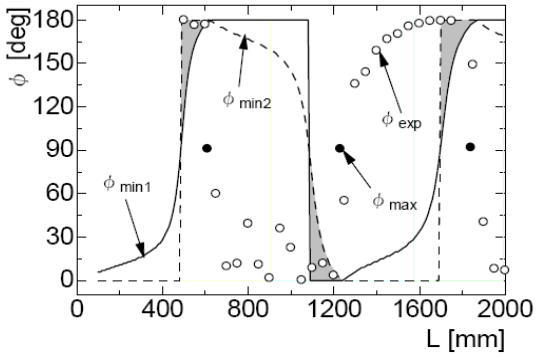

(b) ***When displacement is minimized.***

Fig. 5 ***Theoretical and experimental phase differences between both plate vibrations.***

shaded areas because of decreases in *Lv*1, coinciding with *Lv*2 as *Lpv* peaks. In the acceleration, the motion of plate 1 is almost suppressed by that of the vibrator since the plate 1 is supported by the vibrator, so that α1 is approximately constant in the entire range of *L*. However, since the motion of plate 2 depends greatly on the behavior of the sound field that is the only excitation source for the plate 2, α2 peaks at *L* = 650, 1280, and 1880 mm and is suppressed in the other range of the lengths, like variations in *Lp*1 and *Lp*2. These results reveal that the experimental model cannot completely emulate the theoretical model, whereas it is particular contradiction and the experimental results almost demonstrate the Theoretical phenomena.

4.2. Electricity generation using vibroacoustic coupling

Here, we consider the electricity generation by the plate vibrations coupled to the sound field; the (0,0) mode is adopted as the plate vibration mode, since vibroacoustic coupling between the (0,0) and (0,0,*q*) modes is understood very well on investigation up to the previous section and a decision of the position as to where to attach piezoelectric elements is simple. The mechanical power supplied to the plate 1 by the vibrator can be estimated from the relationship between the point force and the flexural displacement at the excitation point.the acceleration is compare with the point force when it is measured at the respective centers of both plates. Figure 7(a) shows variations in the acceleration α1 and α2 with the point force in the plates 1 and 2, respectively, as the cylinder is removed; the plate vibrations do not couple with the internal sound field. The acceleration should be closely related to the power supplied to each plate, being directly proportional to the respective point forces. In order to understand the circumstances of electricity generation by the piezoelectric elements, Fig. 7(b) shows
the voltages *E*1 and *E*2 generated by the respective plate vibrations as functions of acceleration. *E*1 and *E*2 are also directly proportional to α1 and α2, respectively. These results imply that these voltages are correlated with not only the mechanical power but also the electric power if both powers have directly proportional relationship each other. The effect of vibroacoustic coupling on electricity generation is represented by *E*1 and *E*2 measured in the experimental apparatus with

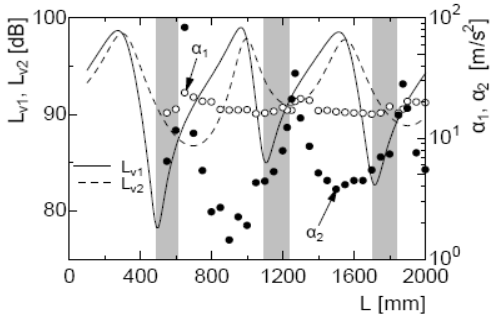

Fig. 6 ***Theoretical vibration levels and experimental acceleration for plates 1 and 2.***

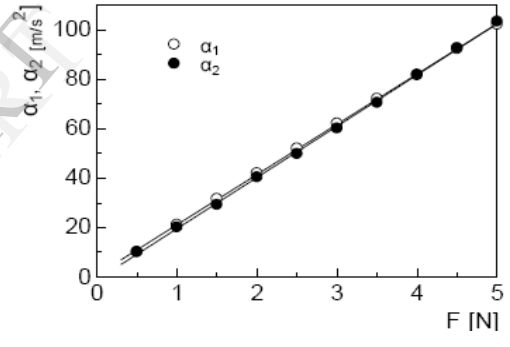

(a) ***Acceleration as a function of point force.***

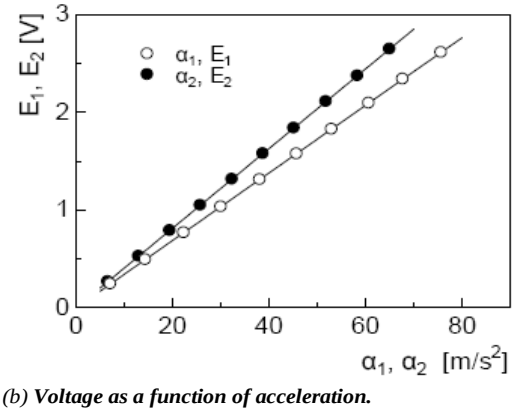

(b) Voltage as a function of acceleration.

Fig. 7 ***Relationship between voltage of electricity generation and plate vibration.***

Although *ER*1 remains almost constant in the entire range of *L*, *ER*2 increases greatly at *L* = 650, 1280, and 1880 mm in the same manner as the vibration levels *Lv*1 and *Lv*2 in Fig. 6. It is natural that the

relationship between *ER*1 and *ER*2 is derived from the reason why *Lv*1 and *Lv*2 behaved. The remarkable results herein are that the acoustic energy based on the sound radiation can be efficiently harvested through vibroacoustic coupling.

5. Conclusion

In order to apply vibroacoustic coupling to electric generation, as one means of harvesting energy from vibration systems, vibroacoustic coupling between plate vibrations and a sound field was investigated theoretically and experimentally for a cylindrical structure with circular end plates, the only one side of which is excited by a harmonic point force. Moreover, the effect of vibroacoustic coupling on the harvest of energy was estimated from the experiment of electricity generation. The present study focused on the condition that amplifies the flexural displacements of the plates and the sound pressure level inside the cavity due to promoting vibroacoustic coupling.

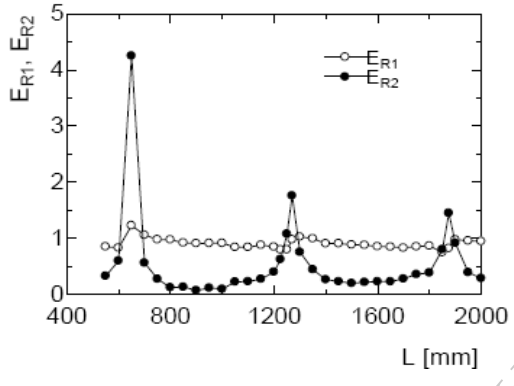

Fig. 8 ***Effect of vibroacoustic coupling on electricitygeneration.***

The theoretical study revealed that the closeness of eigenfrequencies and the similarity of modal shapes are indispensable between the plate vibrations and the sound field to promote vibroacoustic coupling. Such a situation is determined by the dimensions; changes in the cylinder length bring the acoustic mode to shifts in the longitudinal order and also vary periodically the phase difference between both plate vibrations. The experimental results demonstrate the above theoretical estimation in order to amplify the sound pressure level and support complicated acoustic characteristics presumed from the theoretical results. When vibroacoustic coupling is promoted, the experiment of electricity generation verifies that this coupling causes the generation efficiency to increase in comparison with electricity generation caused only by the plate vibration without coupling.

6. References

1. S. Backhaus S. and Swift G. W., ‘‘A thermo acoustic Stirling heat engine,’’ *Nature*, 399, 335–338 (1999).

2.Kitadani Y., Sakamoto S., K. Shibata and Y. Watanabe ‘‘For practical use of loop-tube type thermoacoustic coupling system: discussion about control of the sound field by applying resonance tube,’’ *Proc. Autumn Meet. Acoust. Soc. Jpn.*, pp. 1361–1362 (2010) (in Japanese).

3.Hayamizu K., “Device for electric generation”, Japanese Patent Disclosure 2010-200607 (2010) (in Japanese).

4. Hayamizu K., Ando R. and Takefuji Y., Simultaneous providing device of baseband and carrier signal using sound-generated electricity, *Mobile Multimedia Communications*, No.105-80 (2005-
5), pp.47-49 (in Japanese).

5.Cheng L. and Nicolas J., “Radiation of sound into a cylindrical enclosure from a point-driven end plate with general boundary conditions”, *Journal of the Acoustical Society of America***,** Vol.91, No.3 (1992), pp.1504 1513.

6.Cheng L., “Fluid-structural coupling of a plate-ended cylindrical shell: vibration and internal sound field”, *Journal of Sound and Vibration.* Vol.174, No. 5 (1994), pp.641-654.

7. Larbi, W., Deu, J. F., and Ohayon R., “Finite element formulation of smart piezoelectric composite plates coupled with
acoustic fluid”, *Composite Structures*, Vol.94, (2012), pp.501-509